Available online at www.sciencedirect.com

SCIENCE DIRECT®

Journal of Applied Geophysics 57 (2004) 11–22

JOURNAL OF APPLIED GEOPHYSICS

www.elsevier.com/locate/jappgeo

Granite fracturing and incipient pollution beneath a recent landfill facility as detected by geoelectrical surveys

R. Mota[a,b,*], F.A. Monteiro Santos[b], A. Mateus[c], F.O. Marques[d], M.A. Gonçalves[c], J. Figueiras[c], H. Amaral[e]

[a]*Laboratório Nacional de Engenharia Civil, Av. do Brasil, 101, 1700-066, Lisboa, Portugal*
[b]*Dep. Física and CGUL, Fac. Ciências, Universidade de Lisboa, Edifício C8, Piso 6, 1749-016 Lisboa, Portugal*
[c]*Dep. Geologia and CREMINER, Fac. Ciências, Universidade Lisboa, Edifício C2, Piso 5, 1749-016 Lisboa, Portugal*
[d]*Dep. Geologia and CGUL, Fac. Ciências, Universidade Lisboa, Edifício C2, Piso 5, 1749-016 Lisboa, Portugal*
[e]*Research Project DIWASTE, Fundação da FCUL, Edifício C7, 1749-016, Lisboa, Portugal*

Received 29 November 2002; accepted 12 August 2004

Abstract

A resistivity survey using Wenner array was carried out in June 2000 in a granite region of Northern Portugal, where an active landfill is operating since 1998, to detect the possible spread of contamination. This survey was complemented with a self-potential (SP) survey, a dipole–dipole (DD) array profile and azimuthal Vertical Electrical Sounding arrays (VES). The location of these profiles was highly constrained by the available space in the landfill facility and by the available geological data, mainly fracturing. Significant groundwater circulation was detected, which is characterized by a low resistivity zone (<400 Ω m), with a fairly well defined configuration. Chemical analysis of water samples collected in boreholes inside the landfill facility and on springs around it confirmed the presence of water contamination. The presence of a very well delimited anomaly with low resistivity (<200 Ω m) just beneath the leachate collector system strongly suggests that the groundwater contamination is due to a landfill leak. Results of azimuthal VES are consistent with the structural data obtained outside the landfill, revealing that the strikes of the prevailing fracture systems inside the landfill are generally NW–SE to NNE–SSW, which seems to facilitate the downward propagation of contaminants.

Keywords: Wenner array; Waste disposal; Landfill; Fractured granite; Contaminated groundwater; Azimuthal resistivity

1. Introduction

Disposal in landfills is the most common final destination of domestic and industrial wastes. Landfill sites are usually installed in disused quarries or in specially built facilities. In any case, the need for

* Corresponding author. Dep. Física and CGUL, Fac. Ciências, Universidade de Lisboa, Edifício C8, Piso 6, 1749-016 Lisboa, Portugal.
E-mail address: rpmota@fc.ul.pt (R. Mota).

0926-9851/$ - see front matter © 2004 Elsevier B.V. All rights reserved.
doi:10.1016/j.jappgeo.2004.08.007

strict monitoring and control is in demand, since landfills are potential sources of pollution. Unfortunately, even in controlled facilities problems with contamination spread frequently arise. Thus, almost continuous monitoring is required to detect potential pollution threats. In landfill site investigations, detection and size and shape determination of the polluted area are the usual objectives. Geophysical methods have an important role in assessing those relevant parameters. Chemical composition and physical properties of the waste piles are also important parameters in the evaluation of the environmental impact of the landfills.

Electrical resistivity is the physical property of rocks most affected by the presence of water. The electrical resistivity of the geological basement depends not only on the intrinsic porosity displayed by rocks and sediments at several depths, but also on their air and aqueous fluid content; any variation in underground water chemistry may also affect the electrical properties of the geological basement. Thus, geoelectrical methods are essential tools in the detailed characterization of underground fluid flows. Many different techniques are currently used in conductivity measurements although the electrical method (dc resistivity) is still the most common (e.g., Lima et al., 1995; Dahlin, 1996; Frohlich et al., 1996; Bernstone et al., 2000; Kamura, 2002). The Self-Potential method can be an important complement to the dc method in near-surface groundwater flow detection (e.g., Ogilvy et al., 1969 ;Monteiro Santos et al., 2002) and in geophysical monitoring (Nyquist and Corry, 2002).

This paper deals with the results of a combined geophysical and geological survey carried out at a recent (2 years) landfill facility installed on a homogeneous granitic basement. The main objectives of the study were (a) detection of fracturing in the crystalline basement beneath the landfill, unobservable by geological methods because of the landfill installation, (b) detection of eventual groundwater pollution and estimation of the resulting underground pollution plume extent and, (c) assessment of the azimuthal resistivity method as a tool to study preferential fracture directions in fractured granite massifs.

The geophysical sites and profiles were positioned using data from the geological reconnaissance work. Geological and geochemical data pertaining to this site are reported and discussed in Marques et al. (2001).

2. Geological background

The study area is entirely underlain by a porphyry biotite–granite with homogeneous mineral association and a remarkably uniform whole-rock chemical composition, which in turn is responsible for a fairly constant groundwater chemistry. The thickness of the weathering profile in the granite is usually less than 1 m, but can reach significantly higher values in places where granite fracture density is particularly high or where topography favours colluvium accumulation. In general, the granite does not readily alter to clay minerals; this gives colluvium and soils a sandy texture and results in unsealed granite fractures throughout.

The geological survey covered an area of ca. 100 km^2 around the landfill, and showed that all the area is affected by a conspicuous fracture network (Marques et al., 2001). The apparently low fracture density of some areas is simply due to lack of outcrops. Fractures and faults group in four main subvertical systems, with azimuths N70±15°, N0±5°, N20±10° and N160±10° (Gonçalves et al., 2001). Two distinct slip distributions can be observed on fault surfaces. The gently dipping cluster corresponds to old mineral fibres (mostly quartz) that recorded strike-slip fault movements in Late-Variscan times (Marques et al., 2001, 2002). These faults usually show considerable opening and are thus preferential channel ways for superficial fluid circulation. The steeply dipping cluster represents cold striations carved in clay-gouges; these late movements are correlative of recent uplift and development of an ENE–WSW graben (Marques et al., 2001). The clay gouges of these faults act as dams to underground flow circulation, and accumulation of groundwater against them usually results in local deep weathering of the host granite.

The landfill facility is located on a ridge structurally controlled by subvertical faults striking between N60 and N90. Geological mapping and reconnaissance of the area immediately around the landfill shows that: (i) the landfill was built on the uppermost reaches of a stream watershed that appears to be

Fig. 1. Distribution of the major fractures around the landfill area considering all the fracture clusters identified in the field.

structurally controlled. It coincides with an N–S lineament visible in vertical aerial photographs and digital terrain models (DTMs), but its detailed topographical and geological setting cannot at present be ascertained due to vegetation and landfill covering. (ii) The landfill is very close to densely fractured granite domains located downhill, which is a cause of concern because they may become a big unconstrained pollutant reservoir if reached by contaminated waters. (iii) Around the landfill site, there are many clusters of short, mesoscopic fractures that often appear to be strongly connected (Fig. 1). To the W and SE of the landfill, a significant number of these clusters show high fracture density and comprise open, narrow spaced (<1 m) fractures of prevailing N70±15°, N0±5° and N160±10° directions.

3. Geophysical surveys

Following the main purposes of this study, a geophysical survey took place at the beginning of the dry season in June 2000. Three Wenner resistivity profiles and one dipole–dipole (DD) profile were performed using a multielectrode system from ABEM (Griffiths et al., 1990; Griffiths and Barker, 1993; Dahlin, 1996). Azimuthal Vertical Electrical Soundings (VES) were performed in two different places near the landfill using the Schlumberger array (Masne, 1979; Taylor and Fleming, 1988; Hagrey, 1994; Busby, 2000). The selected sites represent granite domains variably fractured and are located in roughly flat areas in order to minimise topographic effects. Additionally, several Self-Potential (SP) profiles were carried out around the landfill area in order to investigate the probable relationship between SP anomalies and contaminated zones; the four most interesting ones are presented in this paper. Fig. 2 shows the location of the geophysical surveys.

3.1. Wenner and dipole–dipole surveys

Three geophysical lines were set-up in an E–W orientation, using Wenner arrays (profiles W I, W II and W III in Fig. 2). The 360-m-long profile W I was carried out about 150 m north of the dump cell. Profile W II (with a total length of 300 m) was performed close to the southern limit of the dump cell and profile W III (also 300 m long) was carried out about 350 m south of the dump cell. Local topography and

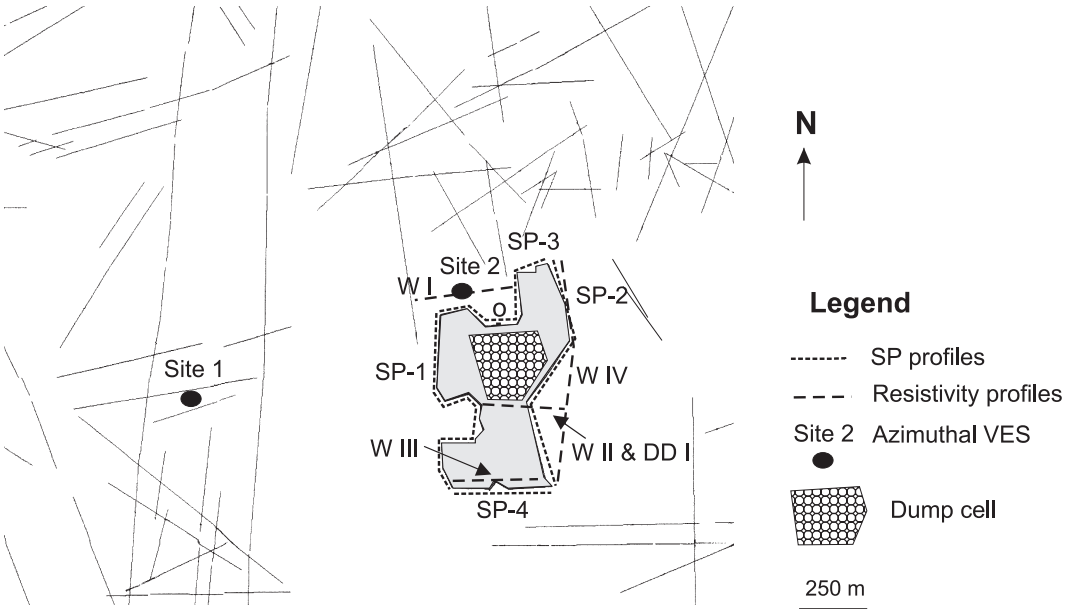

Fig. 2. Location of geoelectrical surveys; the landfill perimeter is also marked to facilitate the comparison with the fracture/fault maps shown above (sites 1 and 2—azimuthal VES; W I to W IV and DD I—resistivity profiles; SP-1 to SP-4—self-potential profiles).

suspected main fault orientation within the landfill constrained the E–W orientation of these profiles. Additionally, a dipole–dipole profile (DD I) was carried out at the same location and with the same length of profile W II. Topographically W II/DD I location is the highest and W III the lowest.

The measured apparent resistivity pseudosections were inverted using the Res2DInv software (version 3.4) (Loke and Barker, 1996). The finite element method was used for the model response calculation (forward modelling) and a combination of the Marquardt and Occam approaches was used for the inversion procedure, with recalculation of the Jacobian matrix after each iteration. Topography data was incorporated into the resistivity models so that topographic effects could be accounted for (Fox et al., 1980; Tsourlos et al., 1999). These effects are very significant in W III and at the western part of W II and DD I.

3.2. Azimuthal VES

This method has been used by several authors to characterize fracture patterns (e.g., Masne, 1979; Taylor and Fleming, 1988; Hagrey, 1994; Carlson et al., 1996a; Hansen and Lane, 1996; Lane et al., 1996; Jansen and Taylor, 1996; Busby, 2000), due to its capability to detect electrical anisotropy, which is related to fracture direction and intensity. This is accomplished by rotating the array about its centre so that the apparent resistivity can be observed in several directions. In a medium with vertical fracturation along the longitudinal reference axis, the diagrams with Shlumberger azimuthal vertical soundings results presents the major axis of the resistivity ellipse aligned with the fracturation, which is a demonstration of the anisotropy paradox (Keller and Frischknecht, 1966; Masne, 1979; Watson and Barker, 1999). It is generally assumed that the observed anisotropy is caused by the presence of fluid-filled fractures in a relatively resistive rock.

In this work, azimuthal VESs were carried out at two sites selected according to the geometry of the main fracture pattern outside the landfill and the probable existence of a main fracture zone within the landfill (Fig. 1). The VESs were carried out for 25 different AB/2 apertures, from a minimum of 1 m to a maximum of 180 m, with the electrodes oriented in four directions (N–S, NE–SW, E–W and SE–NW), which conditioned the angular resolution by 22.5°.

The VES data have been preliminary inverted using a layered-Earth approach (Johanssen, 1977).

3.3. Self-potential profiles

The self-potential (SP) method is based on measurements of the steady state natural electrical potentials existing on the ground surface. As SP electrodes measure the difference in redox potential (geochemical oxidation–reduction reactions) between the reference electrode and the roving one, SP anomalies are due to current flow between different environments and so it can give an indication of the presence of contaminated plume or water flow through rock fractures (e.g., Nyquist and Corry, 2002).

Several SP profiles were carried out around the landfill. The SP measurements were made according to the gradient method, alternating the front and rear electrodes to cancel the electrode polarisation every two measurements. The sampling interval was generally 50 m. Pb–$PbCl_2$ electrodes were used with a digital voltmeter with input impedance of 1 GΩ. Point O in Fig. 2 was used as reference (potential set to zero).

4. Survey results

4.1. Wenner and dipole–dipole surveys

The results obtained are shown in Fig. 3a (Wenner profiles I, II and III) and b (DD I profile). The relative E–W positioning of the inverted resistivity models in Fig. 3a reflects the profile positioning in the field.

The midpoint of azimuthal VES carried out near the landfill is indicated in profile W I. The models reported for Wenner arrays in profiles I to III were achieved after five iterations with an RMS error of 2.3, 4.1 and 3.7, respectively. The DD profile inversion converged after four iterations with an RMS error of 12.3.

The model obtained for profile W I shows a low resistivity anomaly (<400 Ω m), which goes deep and starts roughly around 8 m beneath the topo-

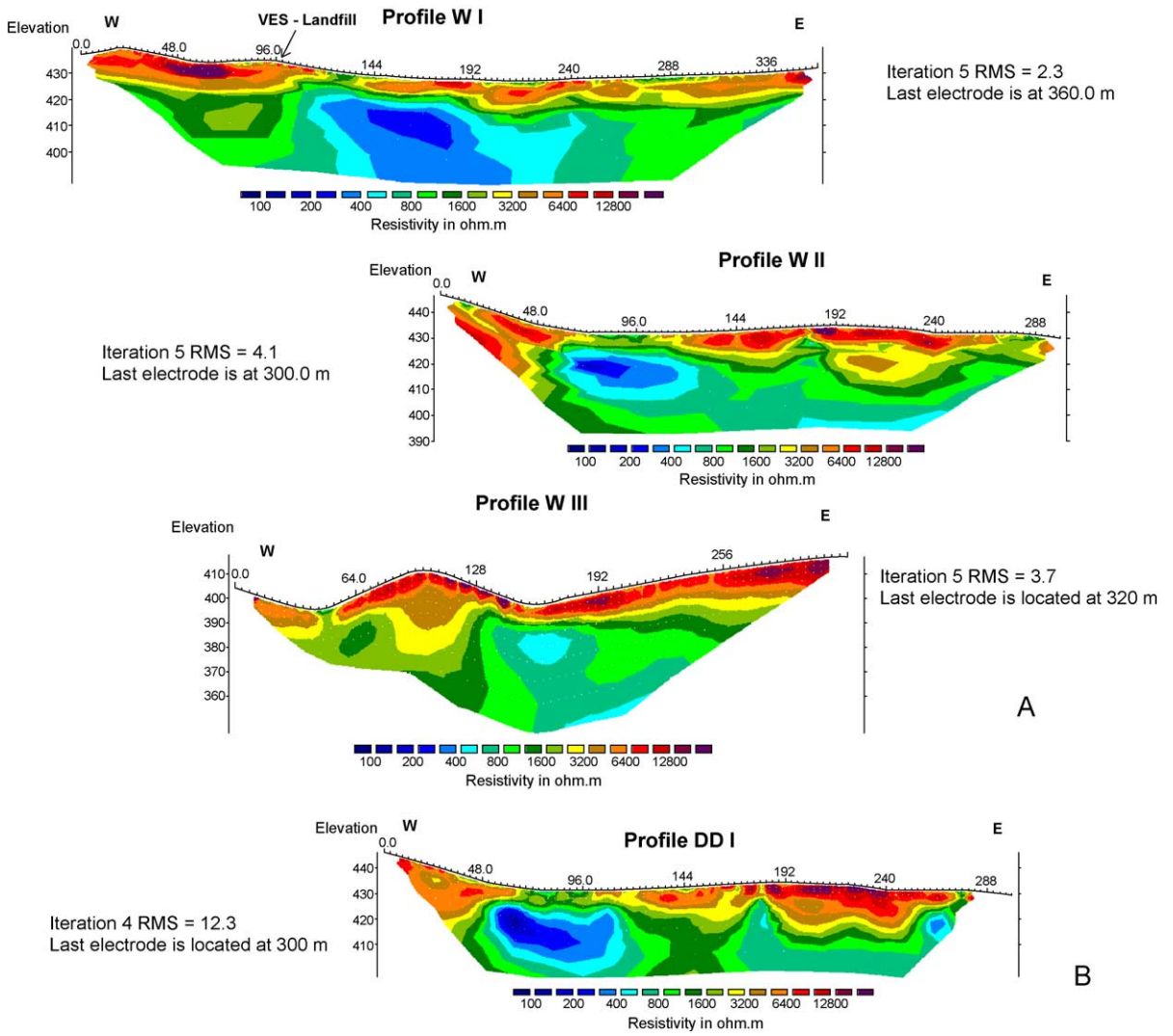

Fig. 3. Geoelectrical models considering the effects of topography obtained from inversion of the Wenner data—profiles W I to III (A) and dipole–dipole data (B). Models W I to W III are aligned such that a straight vertical line through all defines an N–S line in the map of Fig. 2. Vertical exaggeration for all models is 1.23. Unit electrode spacing is 3.0 m for all profiles, except profile W III, where it is 4.0 m.

graphic surface. Near the western end of profile W I, there is a small, although intermittent, water spring; in winter, the soil is always evidently wet close to the profile point 144. The low resistivity anomaly seen in W III also coincides with a perennial small creek. No surface geological recognition can be performed at the W II and DD I locations because of the engineering works done for the landfill installation. The western part of these profiles is located on a large, lightly fractured granite outcrop that corresponds to the deepest and most resistive overburden obtained. However, a well-defined low resistivity anomaly can be seen in these profiles (Fig. 3). This anomaly develops just beneath the pipe of the leachate collector system (roughly below point 96), and is much more circumscribed in depth than those seen in profiles W I and W III, although sensitivity tests showed that it is not well constrained in depth.

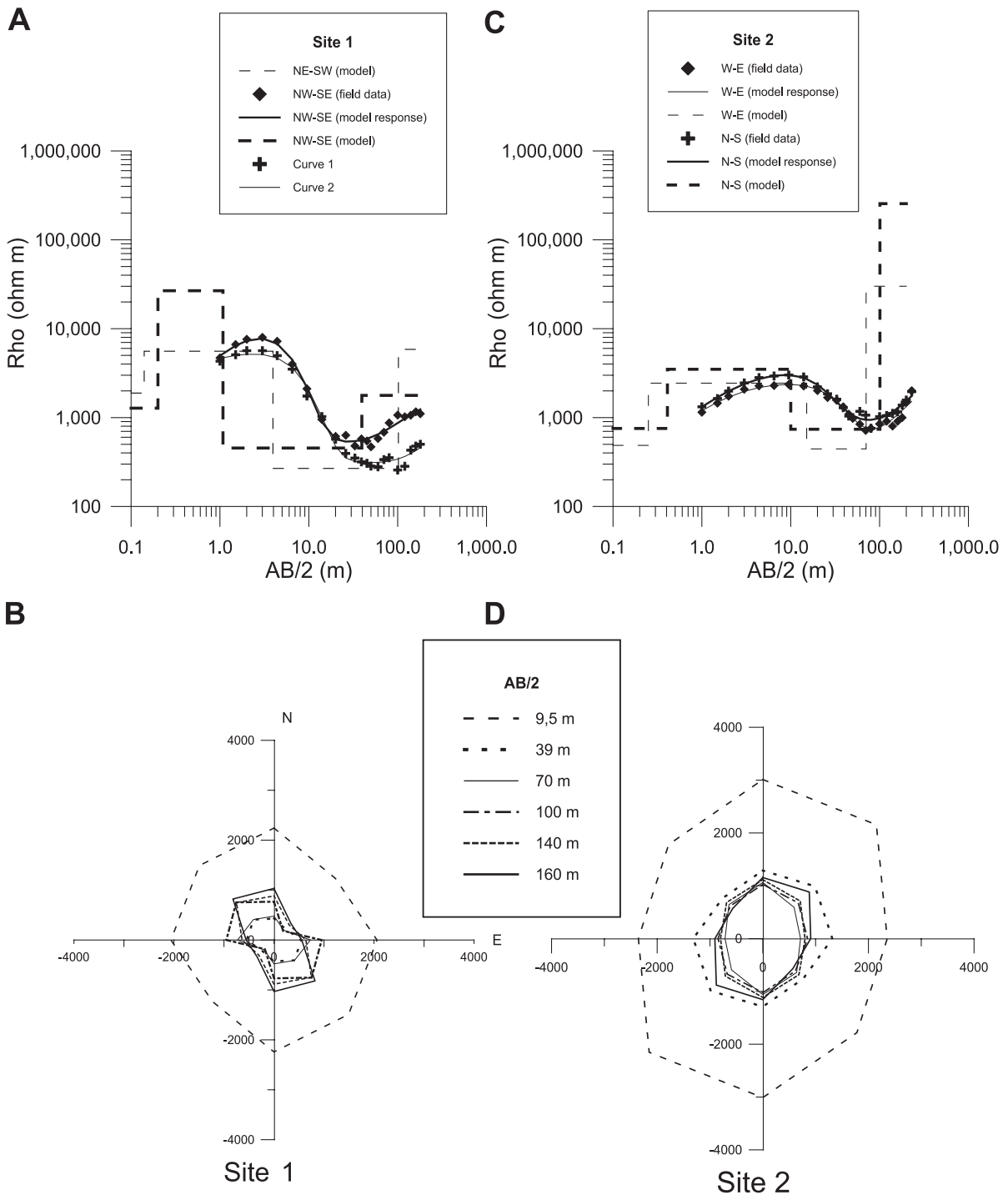

Fig. 4. (A, C) Orthogonal apparent resistivity curves obtained at sites 1 and 2 (dots), model response (lines) and models (dashed lines). (B, D) Azimuthal VES apparent resistivity results at selected AB/2 distances.

It should be emphasised that models for Profiles W II and DD I obtained from Wenner and DD data inversion match quite well, the low resistivity anomaly being more contrasting in the model corresponding to the DD array.

4.2. Azimuthal VES

Fig. 4a and c shows the apparent resistivity data obtained from soundings carried out in two orthogonal directions at site 1 (900 m west of the landfill and at 450 m asl) and site 2 (located close to the landfill, at 436 m asl), respectively. Fig. 4b and d shows the azimuthal resistivity results obtained at sites 1 and 2 for some selected AB/2 distances.

The obtained inversion models are presented in Fig. 4a and c to compare the model response with the field data. The fit between them is acceptable since misfits are generally lower than 10%. An isolated misfit value of 30% occurs at site 1 in the NE–SW direction. As can be seen, both sites can be modelled as a stacking of four different layers, more resistive and less resistive layers alternating down the profiles. The top layer is very thin and discontinuous and the bottom one is poorly resolved during the inversion procedure, because only a few data points are influenced by its properties.

The low resistivity layer at each site (the third layer) has a conductance ($S=h/\rho$) of 0.38 S (NE–SW) and 0.09 S at site 1, and 0.14 S (N–S) and 0.16 S at site 2.

Fig. 5 shows the anisotropy coefficient, λ, calculated from the apparent resistivity curves corresponding to the ellipse's principal directions, using the following relation:

$$\lambda = \sqrt{\frac{\rho_y}{\rho_x}} \tag{1}$$

(ρ_y—apparent resistivity measured along the ellipse major axis direction; ρ_x—apparent resistivity measured along the ellipse minor axis direction).

At site 1, the highest λ value (about 2.0) is found for an AB/2 spacing of 100 m. The calculated λ values are much lower at site 2. Their maximum value, 1.2, is obtained for AB/2 spacings ranging from 50 to 70 m.

4.3. Self-potential profiles

The results from four SP-profiles carried out around the landfill are presented in Fig. 6 together with topography levels and will be discussed in the next section.

Profile SP-1, which follows the western border of the landfill area, shows negative SP values with a relative maximum at coordinates 200–250 m after a local minimum. Minimum SP values (−120 to −150 mV) occur at coordinate 500 m. This local minimum is followed by an increase of the SP values.

Profile SP-2 performed along the eastern border of the landfill shows maximum SP values (positive values) around coordinate 200 m, which corresponds to the point of the profile with the highest topographic elevation. The minimum values on the SP potential (−30 to −50 mV) are reached at coordinate 550 m.

In profile SP-3, acquired in the northern part of the landfill area, the most significant variation appears around coordinate 400 m.

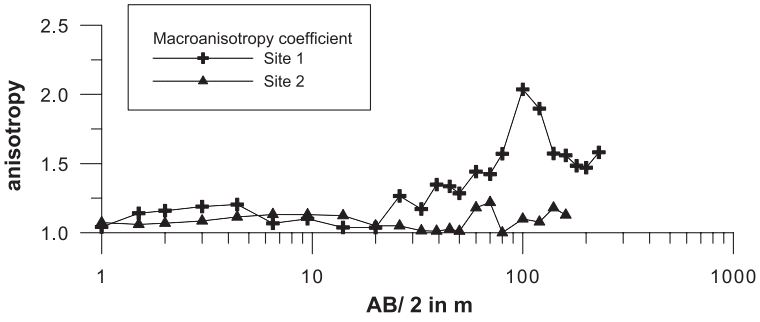

Fig. 5. Anisotropy coefficient versus electrode spacing obtained at sites 1 and 2.

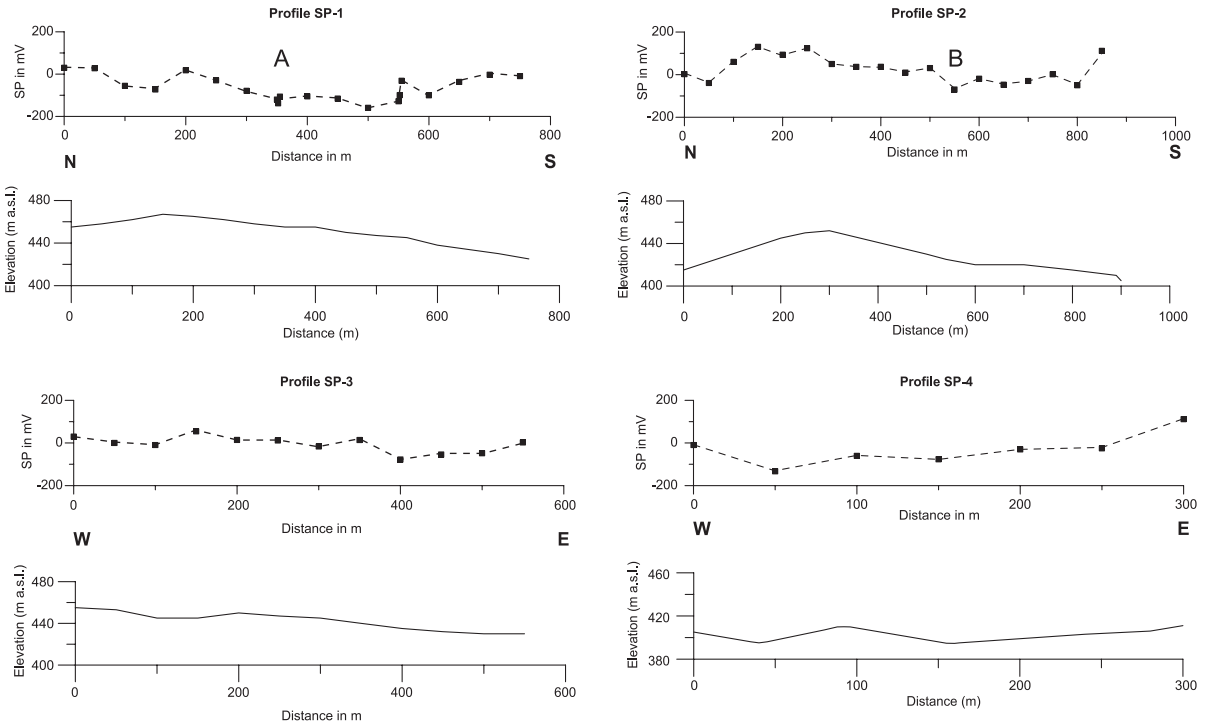

Fig. 6. Self-potential profiles carried out in the vicinity of the landfill facility. Measurements A and B in the profiles SP-1 and SP-2 were performed in the W–E direction (see also Fig. 2).

Profile SP-4 was performed along the south border of the landfill, with a length of 300 m. This profile was affected by high topographic variations.

5. Interpretations and discussion of results

In all models, the overburden resistivity is generally above 6400 Ω m with a maximum thickness of 5 m, thus correlating quite well with superficial dry granite. The basement usually presents a resistivity of 1600 Ω m. This resistivity contrast must reflect the different electrical response of dry and wet granite, respectively. Apart from this surface-depth contrast, all profiles are dominated by the presence in their central–western zone of a deep-lying low resistivity anomaly. High resistivity deep domains, most prominently the one seen at the western tip of profiles W II/DD I, are relatively unfractured (and thus, unaltered and dry) granite domains, as it was seen in the geological survey. Several such domains outcrop at all scales across the region, the ridge whereon the facility is built being itself a very large scale of such comparatively unfractured and unaltered domain.

The deep central–western low resistivity anomaly seen in the profiles has no straightforward geological interpretation. In profiles W II/DD I and W III, this anomaly is located beneath a former creek that aerial photograph interpretation and DTM examination show must have carved the ridge side along a fracture zone; however, there is no geological reason why this fracture zone should have significantly higher fracture density or water contents than the rest of the vertical fracture zones seen in the eastern parts of the profiles, thus explaining its lower resistivity. In profile W I, the anomaly is to the west of the creek just mentioned, but may be also installed in an NNW–SSE fracture zone, for which there is faint geological evidence expressed as an incipient seasonal rivulet that crosses W I over the anomaly, and as a set of recognized fractures parallel to the one believed to host the anomaly.

Moreover, the character of the anomaly varies from profile to profile. In profiles W II/DD I, the resistivity falls to very low values (<400 Ω m). In profile W I,

the anomalous zone is clearly not confined in depth and its lateral limits are much more diffuse than in profiles W II/DD I. In profile W III, the anomaly, although clearly recognizable has central resistivity values barely below those of the geophysical background. The anomaly is thus very circumscribed and intense under profiles W II/DD I, it spreads in depth and to the northwest until it crosses profile W I and is almost lost to the south before intersecting profile W III. In a work performed in a similar geological environment, Frohlich et al. (1996) found similar values with Vertical Electrical Soundings using Schlumberger array, for water filled fractures.

In the absence of any evidence, whatever for the presence of special circumscribed domains within the granite massif, the low resistivity anomaly being discussed must be interpreted as resulting from the presence of a low resistivity fluid, the most obvious candidate being waste leachate diluted by groundwater. The leachate probably would leak from the facility in the vicinity of profiles W II/DD I as this profile is at the highest topographic level, crosses the leachate collector system roughly under point 96 of the profile and has the more confined anomalous zone, and spread horizontally (and, to a certain extent, also vertically) to the northwest along one or several fracture zones. Sensitivity tests showed that the anomaly in profiles W II/DD I is not well constrained in depth; therefore, one have to analyse the possibility of vertical flow. In the north–south fracture zone that seems to coincide with the former creek in which the upper watershed facility was built, there is some obstacle to the vertical spreading of the leachate. Outcrop conditions preclude the geological detection of deep lying horizontal fracture zones. From the geology, it is impossible to determine if the obstacle to vertical spreading is a geological feature or just the normal closure of open fractures in depth. In any case, the spread of the leachate contamination is limited downward to around 410 m asl. As profile W III lies entirely below this elevation, it is to be expected that the contaminated waters would have escaped to the surface before reaching this profile W III, resulting in a very faint low resistivity anomaly in this profile, as observed, and in the chemical pollution of the perennial creek which crosses the profile at point 158. Indeed, chemical analysis of this creek water reveals high concentrations above background of several metals and nonmetals, most notably Al, Mn, Fe, Cu and Zn.

In what concerns the azimuthal VES results, a simple comparison with the fracture network maps shows that the strike of the prevailing, hydraulically conductive, fracture systems is coarsely normal to the minor ellipses axes for all the AB/2 spacings used, as already stated by other authors (e.g., Masne, 1979; Taylor and Fleming, 1988; Hagrey, 1994; Watson and Barker, 1999; Busby, 2000). An N–S dominant direction can be deduced for the VES set located in the landfill vicinity (site 2). From the azimuthal VES carried out at site 1, a predominant NW–SE direction for the fracture/fault zones can be inferred, although the axial ratio of the obtained ellipse suggests that other fracture systems can be present, particularly if data for small AB/2 spacing is considered. This can be correlated with the available geological measurements for the selected site, whose higher fracture density records the development of a complex fracture network composed of several systems with distinct directions (Fig. 1).

At depth, resistivity is lower at site 1 than at site 2. The possible explanation for this is the higher level of fracturation at site 1(Fig. 1), with a higher content of water. Near site 1 is the probable spring of Reamondes river.

A consistent azimuthal pattern can be observed at sites 1 and 2 for AB/2 greater than 10 m and it can be interpreted as originated from the geological fracturing. At site 1, the results suggest that there is a dominant fracture set approximately in the NW–SE direction. At site 2 however, the results indicate a main fracture set approximately in the N–S direction. These results suggest that the geological medium might be more uniformly fractured in the vicinity of site 2 comparatively to site 1.

In the SP method, the magnitude of the potential depends on several factors, mainly electrical conductivity of the fluid and its dynamic viscosity. Dielectric constant and zeta potential at the rock/fluid interface are also parameters that influence the potential magnitude. SP potentials related to redox reactions are also frequently mentioned in the literature. All these dependencies made quantitative interpretations very difficult. Also, the values of SP are very often correlated with significant elevation differences, further complicating their interpretation in terms of

fluid flow. Therefore, only a qualitative interpretation is made in this work. The major variations in SP-2 profile values are probably due to topographic effects. Negative SP values can, though, be related to the presence of contaminants transported by surficial water flow.

The topographic effects seem not to be significant in profile SP-3 and the SP anomaly can be interpreted as resulting from in situ contamination enrichment made easy by the fracturation already interpreted on the basis of the lineament that crosses the landfill area approximately in the NNE–SSW direction. In contrast, the values measured along profile SP-4 are strongly affected by topographic effects, and their correlation with geological features or fluid flow becomes very difficult. However, in accordance with the results obtained from geoelectrical profile W III, the fault just referred to must cross the SP-4 profile in the vicinity of the coordinate marked with A. Because no high thermal gradient field or core bodies are known in the study zone, electrokinetical effects connected with subsurface flows are the most probable cause for SP anomalies.

The commonly observed unaltered granite outside the landfill is the result of Quaternary uplift (Cabral, 1989) and restricted water percolation, which indicates that porosity is very low and, thus, that the granite is dry. This means that water circulation is taking place in fractures rather than through pores. Therefore, when geoelectrical surveys show low resistivity zones we interpret them as fractured granite being percolated by water, which may come from the landfill installation since geophysical study was carried out during the summer.

6. Conclusions

The combined interpretation of the fracture maps and geoelectrical results indicates that the granite in the NW part of the study area is strongly fractured mainly in directions ranging from NNW–SSE to NNE–SSW. At the southwest part of the landfill, the resistivity models (from profiles W II and DD I) display high resistivity values corresponding to low fractured and dry granite.

Combining the available results, we may conclude that there is groundwater contamination by the accumulation of leachate in a fractured zone located in the vicinity of the collector system, as detected in profiles W II/DD I. Groundwater is moving north and southwards in accordance with the topography of the area. The contaminated flow is identified to the north of the landfill in profile W I and at south superficially in the creek and more diffuse at depth in profile W III.

Acknowledgments

The authors express their appreciation to the landfill exploration company for the unrestricted access consent. Thanks to LNEC are also due for fieldwork support. Important and constructive reviews were made by R.K. Frohlich and S.A. al Hagrey and by the Editor A. Hördt. This work is a contribution of the research project DIWASTE (PRAXIS/P/CTE/11028/1998) funded by FCT/MCT and FEDER.

References

Bernstone, C., Dahlin, T., Ohlsson, T., Hogland, W., 2000. DC-resistivity mapping of internal landfill structures: two pre-excavation surveys. Environ. Geol. 39, 360–371.

Busby, J.P., 2000. The effectiveness of azimuthal apparent-resistivity measurements as a method for determining fracture strike orientations. Geophys. Prospect. 48, 677–695.

Cabral, J., 1989. An example of intraplate neotectonic activity Vilariça Basin, Northeast Portugal. Tectonics 8, 285–303.

Carlson, D.A., Taylor, R.W., Cherkauer, D.S., 1996. Azimuthal resistivity as a tool for determination of the orientation of preferred hydraulic transmissivity for a dolomite aquifer in Southwestern Wisconsin: SAGEEP 1996 Conference. Environ. Eng. Geophys. Soc. Proc., 1085–1094.

Dahlin, T., 1996. 2D resistivity surveying for environmental and engineering application. First Break 14, 275–283.

Fox, R.C., Hohmann, G.H., Killpacks, T.J., Rijo, L., 1980. Topographic effects in resistivity and induce-polarization surveys. Geophysics 45, 75–93.

Frohlich, R.K., Fisher, J.J., Summerly, E., 1996. Electric-hydraulic conductivity correlation in fractured crystalline bedrock: Central Landfill Rhode Island, USA. J. Appl. Geophys. 35, 249–259.

Gonçalves, M.A., Amaral, H., Mateus, A., Marques, F.O., 2001. Fracture density and scaling laws in granite massifs and their importance on site selection criteria for waste disposal. Annual Conference of the International Association for Mathematical Geology. Cancún, Mexico.

Griffiths, D.H., Barker, R.D., 1993. Two-dimensional resistivity imaging and modelling mapping in areas of complex geology. J. Appl. Geophys. 29, 211–226.

Griffiths, D.H., Turnbull, J., Olayinka, A.I., 1990. Two-dimensional resistivity mapping with a computer-controlled array. First Break 8, 121–129.

Hagrey, S.A., et al., 1994. Electric study of fracture anisotropy at Falkenberg, Germany. Geophysics 59, 881–889.

Hansen, B.P., Lane, J.W., 1996. Orientation and characteristics of fractures in crystalline bedrock determined by surface and borehole geophysical surveys, Millville and Uxbridge, Massachusetts: SAGEEP 1996 Conference. Environ. Eng. Geophys. Soc. Proceedings, 927–940.

Jansen, J., Taylor, R., 1996. Determining fracture geometry from azimuthal resistivity data: SAGEEP 1996 Conference. Environ. Eng. Geophys. Soc. Proc., 41–50.

Johanssen, H.K., 1977. A man/computer interpretation system for resistivity soundings over a horizontally stratified earth. Geophys. Prospect. 25, 667–691.

Kamura, K., 2002. Relationships between electrochemical properties of leachate and resistivity of strata in the landfill site consisting mainly of combustion residuals. Environ. Geol. 41, 537–546.

Keller, G.V., Frischknecht, F.C., 1966. Electrical Methods in Geophysical Prospecting. Pergamon Press.

Lane, J.W., Haeni, F.P., Soloyanis, S., Placzek, G., Williams, J.H., Johnson, C.D., Muursink, M.L., Joesten, P.K., Knutson, K.D., 1996. Geophysical characterization of a fractured-bedrock aquifer and blast-fractured contaminant-recovery trench: SAGEEP 1996 Conference. Environ. Eng. Geophys. Soc. Proc., 429–441.

Lima, O.A.L., Sato, H.K., Porsani, M.J., 1995. Imaging industrial contaminant plumes with resistivity techniques. J. Appl. Geophys. 34, 93–108.

Loke, M.H., Barker, R.D., 1996. Rapid least-squares inversion of apparent resistivity pseudosections by a quasi-Newton method. Geophys. Prospect. 44, 131–152.

Marques, F.O., Mateus, A., Amaral, H., Gonçalves, M.A., Tassinari, C., Silva, P., Miranda, J.M., 2001. The Amares basin: an ENE–WSW graben formed by recent reactivation of the Late-Variscan fracture network? Comun. Inst. Geol. Min., Tomo 88, 33–50.

Marques, F.O., Mateus, A., Tassinari, C., 2002. The late Variscan fault network in Central–Northern Portugal (NW Iberia): a re-evaluation. Tectonophysics 359, 255–270.

Masne, D., 1979. Application de methods electriques et electromagnetiques a l'étude geophysique des millieux fissures. These 3ème Cycle. Université des Sciences et Techniques du Languedoc.

Monteiro Santos, F.A., Almeida, E., Castro, R., Nolasco, R., Mendes-Victor, L., 2002. A hydrogeological investigation using EM34 and SP surveys. Earth Planets Space 54, 655–662.

Nyquist, J.E., Corry, C.E., 2002. Self-potential: the ugly duckling of environmental geophysics. The Leading Edge, 446–451.

Ogilvy, A.A., Ayed, M.A., Bogolovsky, V.A., 1969. Geophysical studies of water leakages from reservoirs. Geophys. Prospect. 17, 36–62.

Taylor, R.W., Fleming, A.H., 1988. Characterizing jointed systems by azimuthal resistivity surveys. Ground Water 26, 464–474.

Tsourlos, P.I., Szymanski, J.E., Tsokas, G.N., 1999. The effect of terrain topography on commonly used resistivity arrays. Geophysics 64, 1357–1363.

Watson, K., Barker, R., 1999. Differentiating anisotropy and lateral effects using azimuthal resistivity offset Wenner soundings. Geophysics 64, 739–745.